Acta Scientiarum

http://periodicos.uem.br/ojs
ISSN on-line: 1807-8664
Doi: 10.4025/actascitechnol.v44i1.58660

Grid-connected photovoltaic system to mitigate momentary voltage dip based on the balance between the active and reactive powers

Anderson Rodrigo Piccini[1, 2*], Geraldo Caixeta Guimarães[1], Arthur Costa de Souza[3], Ana Maria Denardi[2], Leonardo Rosenthal Caetano Silva[4] and Jaqueline Oliveira Rezende[1]

[1]Faculdade de Engenharia Elétrica, Universidade Federal de Uberlândia, Uberlândia, Minas Gerais, Brasil. [2]Instituto Federal de Educação, Ciência e Tecnologia do Paraná, Rua José Felipe Tequinha, 1400, 87703-536, Paranavaí, Paraná, Brasil. [3]Universidade Federal de Itajubá, Itabira, Minas Gerais, Brasil. [4]Instituto Federal de Educação Ciência e Tecnologia de Goiás, Itumbiara, Goiás, Brasil. *Author for correspondence. E-mail: anderson.piccini@ifpr.edu.br

ABSTRACT. With a great potential yet to be explored in Brazil, the grid-connected photovoltaic system, besides supplying the active power, can also contribute to improve the voltage level grid providing reactive power. Therefore, this work proposes to use a Grid-Connected Photovoltaic System (GCPVS) equipped with a control that uses the automatic voltage regulator (AVR) to balance the injection of the active and reactive powers, thus softening the short-duration voltage variation, more specifically the momentary voltage dip. For this purpose, the GCPVS was connected in part of a real distribution grid that attend the block 1106 South of Palmas city, state of Tocantins, northern region of Brazil. It is shown that the active and reactive power delivered to the grid can be controlled to help the power quality of the main grid during a disturbance. During a short-circuit situation, the active power is reduced, freeing up space from the inverter capacity for maximum supply of reactive power, in this way, helping the main grid to return to an adequate voltage level. The simulation results show that such voltage profile improvement is possible. Therefore, they confirm that photovoltaic systems, even though considered small, can also provide ancillary services to the low voltage distribution grid during abnormal conditions, adding to the actions normally performed by conventional power plants.

Keywords: Short-duration voltage variation; momentary voltage dip; grid-connected photovoltaic system; balance between the active and reactive powers; automatic voltage regulator.

Received on April 14, 2021.
Accepted on October 1, 2021.

Introduction

Distributed Generation (DG) can be defined as a source of electricity generation connected directly to the distribution grid, close to the point of consumption, regardless of the source of energy or fuel, the power or the size of the generating unit and, finally, the technology involved (Agência Nacional de Energia Elétrica [ANEEL], 2018a; Instituto Nacional de Eficiência Energética [INEE], 2020). Because of these characteristics, DG continues to gain significant interest among companies and end consumers of electricity around the world.

DG technologies have quickly evolved to include ever-lower powers. In this evolution, all the equipment involved, such as measurement, control and command (whose purpose is to articulate the operation of generators) and the eventual control of loads (on/off) must, at the same time, adapt to the systems and energy supply (Albuquerque, Moraes, Guimarães, Sanhueza, & Vaz, 2010; Piccini, Tamashiro, Rodrigues, Guimarães, & Barbosa, 2014; Piccini, Guimarães, Souza, & Denardi, 2021). Among the DG systems, those referred as Renewable Energy (RE) sources (wind, solar, biomass and landfill gas) have aroused great interest, due to their variety, environmental concerns, increased demand for electricity and support for utility grids (Goqo & Davidson, 2018; Kabalcı, 2020).

Among the renewable sources, the photovoltaic solar energy has stood out, due to its increasing deployment and market share. As a result of the growing adoption of this resource, the electric distribution Grid-Connected Photovoltaic Systems (GCPVS) is developing at an amazingly fast pace and will soon be a large part of power generation in some regions. Given this fact, there are changes in dynamic behavior and impacts in this distribution grid, where such system has been inserted (Afshari, Moradi, Yang, Farhangi, & Farhangi, 2017; Goqo & Davidson, 2018; Sufyan, Rahim, Eid, & Raihan, 2019).

In addition, some incentive rules and regulations are introduced by governments to increase the RE penetration in the energy matrix of each country, which is connected to the low and medium voltage distribution grids such as DG (Ammar & Sharaf, 2019; Mishra & Lal, 2020). Because of this greater use, the operation of the distribution grid with the participation of DG has been researched with interest. Especially when it comes to this participation in voltage control in a permanent regime and the benefits that can be included, such as increased hosting capacity, reduction in voltage fluctuation and load reduction, using these RE technologies connected DG in the local distribution grid (Ammar & Sharaf, 2019).

To this end, researchers are exploring Photovoltaic System (PVS) not only as active power suppliers, but also as reactive power suppliers (Al-Shetwi, Sujod, & Blaabjerg, 2018; Mishra & Lal, 2020; Sufyan et al., 2019). According to the previous version of IEEE 1547, 2003, at the point of interconnection, DG (including photovoltaic solar energy generators) cannot actively participate in voltage regulation, controlling the reactive power in the grid (Mishra & Lal, 2020). From the update and approval of IEEE 1547-2018, the distributed generators can now participate in the mains voltage support actively, thus, they are able to provide reactive power compensation (Institute of Electrical and Eletronics Engineers [IEEE], 2018). It is worth mentioning that, at the moment, the Brazilian regulation has not allowed this compensation yet, but it is expected that the international standard will soon be adapted, through public consultations established by ANEEL.

Several publications related to the integration of photovoltaic systems into the distribution grid were presented. Along with them, some methods for active and reactive power management and control were being discussed. It is worth noting that the control of reactive power is one of the important requirements for the distribution grid voltage stability. Some of the most recent methods of controlling reactive power will be presented. One of the methods was discussed by (Safayet, Fajri, & Husain, 2017), which has as a characteristic the efficient use of reactive power management when connected to a critical bus in the distribution grid. The method increases voltage regulation and improves the reverse flow of energy of a distribution system with high penetration of RE sources, while it efficiently uses the reactive power capacity of the photovoltaic inverter.

To solve the problems of overvoltage on the DC bus and overcurrent on the AC side, (Al-Shetwi et al., 2018) discussed a control strategy to improve Low Voltage Ride Through (LVRT) capability at the single-stage photovoltaic plant based on Malaysian standards. This control also proposes to solve the problems that cause disconnection or damage to the inverter and only reactive power injection during symmetrical and asymmetric faults. On the other hand, the work presented by (Wen & Fazeli, 2019) describes a strategy of LVRT control for three-phase low voltage GCPVS, in which, based on the capacity of the inverter to remain connected during voltage dip and during asymmetric faults, the inverter injects sinusoidal current up to twice its rated current. Even when the fault occurs, the control prevents the performance of the maximum power point tracking (MPPT) by switching to an algorithm that does not use this technique, but that guarantees a smooth transition between the two methods (with and without MPPT). In addition, the reference (Wen & Fazeli, 2019), highlights Brayton – Moser's mixed potential theory and injects only reactive power during faults.

Finally, to demonstrate the relevance of the subject that deals with the compensation of reactive power in the distribution grid, (Mishra & Lal, 2020) proposes a mathematical methodology to derive the active and reactive power capacity curve of a photovoltaic system integrated into the grid. Also managing the injection of reactive power into the grid in its maximum power condition for various environmental conditions. With this, it was possible to determine the reactive power limits for single and three-phase systems connected to the IEEE 33-bus distribution grid.

Although the previous methods are able to provide reactive power, they have disadvantages of several additional components that incur additional costs and due to they do not address the problem of energy balance during the voltage sag. However, in the application of the GCPVS based on single stage inverter, so far, few papers have sufficiently covered a comprehensive strategy to cover the voltage sag while providing balanced reactive power with active support to the grid. Therefore, the main purpose of this work is to propose an optimization in the control for a low voltage three-phase GCPVS that can contribute to ancillary services.

Thus, an improvement of the reactive power injection control is presented in order to help to sustain the voltage in the PCC (Point of Common Coupling) during the short-duration voltage variation (SDVV), more specifically, the momentary voltage dip (MVD). In this way, the control contributes to support the voltage level of the grid using the strategy of the automatic voltage regulator (AVR). For this purpose, the AVR parameters will be modified to faster dynamics, thus identifying the short-duration voltage variation. To mitigate the effects of the fault, the GCPVS must remain connected into the grid, balancing the powers, decreasing the injection of active power and injecting the maximum reactive power available, in view of its

total capacity to help to support the voltage levels of the grid. This GCPVS was implemented on the Matlab/Simulink® computational platform, in a real electric distribution grid in the city of Palmas, which is located in the state of Tocantins, in the northern region of Brazil.

In relation to the other aforementioned methods, this improvement seeks to optimize and balance the best amount of injection of active and reactive power at the time of fault, using the idea of the AVR and modifying the phase angle of the output voltage. Thus, decrease the injection of active power and increase the injection of reactive power at the time of MVD. Thus, once the disturbance is eliminated, all values return to the pre-fault condition and only the active power is injected into the grid, as shown in Figure 1.

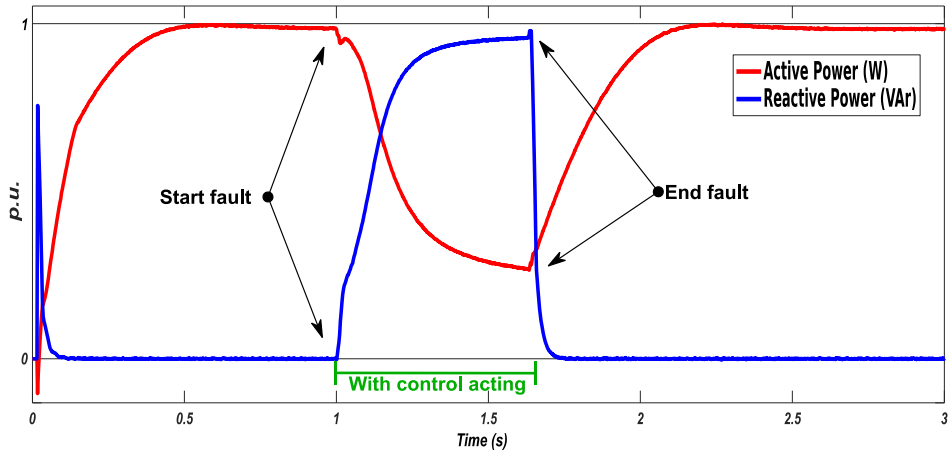

Figure 1. Proposed enhancement to balance the injection of active and reactive power into the power grid.

Material and methods

For this study, a GCPVS was modeled without the use of the boost voltage converter, which has the function of raising/adjusting the voltage of the photovoltaic arrangement for the photovoltaic inverter. This one is also known as a single-stage converter. The model was characterized by a photovoltaic arrangement of 75 kW, with 21 modules in series and 9 strings in parallel, the modules are from Jinko Solar model JKM400M (Jinko Solar, 2020), (respecting the characteristics presented and suggested by (Comerio, Scarpart, Krause, Fernandes, & Muniz, 2020; Michels et al., 2015)), combined with the MPPT technique applied directly to the inverter. In addition, three-phase inverter and, finally, the LCL filter (inductive-capacitive-inductive) that connects to the low voltage distribution grid.

The three-phase photovoltaic inverter with VSI (Voltage Source Inverter) topology is used to perform the energy conversion and for the purpose of optimization of the control. The control structure of the inverter meets all the specifications of national and international technical standards and it is especially compatible with the technical standards required by ANEEL ("Agência Nacional de Energia Elétrica" – National Electrical Energy Agency), specifically by guidelines of PRODIST ("Procedimentos de Distribuição" – Distribution Procedures) for SIN ("Sistema Interligado Nacional" – National Interconnected System). They are regulatory standards in Brazil (ANEEL, 2021).

For MPPT control, there are several different methods of tracking, as presented by (Caetano et al., 2019). Among all the techniques offered by the mentioned authors, the method used in this proposal was the Perturb and Observe (P&O) technique, due to its reliability, practicality and capacity to deliver the maximum power to the grid together with the active and reactive power control of the inverter (Al-Shetwi et al., 2018). It also uses the P&O algorithm with integrated regulation that has a switching frequency of 8 kHz linked to the inverter switches. It should be noted that the voltage on the DC bus corresponds to 875.7 V, while on the AC grid side it corresponds to a line voltage of 380 V at 60 Hz.

In this work, the switching frequency used for the inverter was PWM pulse width modulation (Pulse Width Modulation) at 8 kHz. At the output of the inverter, an LCL filter is inserted for each phase, where these third-order coupling filters are responsible for filtering and connecting the inverter to the power grid (Reznik, Simões, Al-Durra, & Muyeen, 2014; Teodorescu, Liserre, & Rodriguez, 2011). The inverter control block diagram is shown in Figure 2. This control has a current control loop, a voltage and active power control loop, another reactive power loop and a PLL (Phase Locked Loop) reference synchronous.

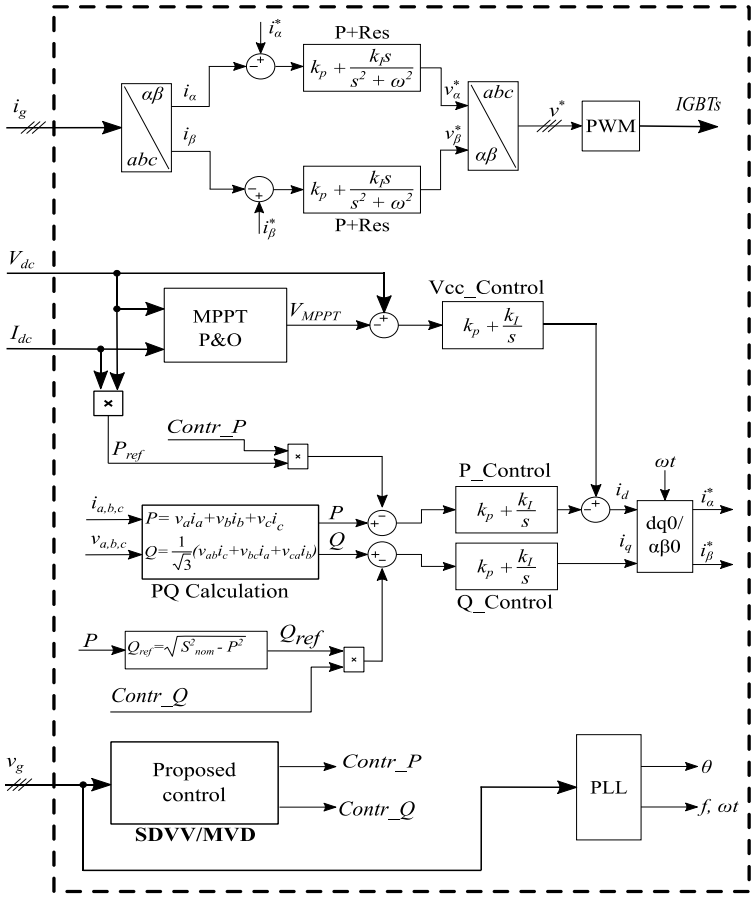

Figure 2. Block diagram of the inverter with proposed control.

For the current control loop, the damped proportional resonant compensator (P + Res) was used, according to Equation (1), which operates in the stationary frame of reference (*αβ0*), which was presented by (Teodorescu et al., 2011). The output of this control is sent to the PWM pulse distribution unit. It is worth mentioning that the voltage control loop is also known as the power loop, since the voltage regulation of the DC bus indirectly seeks to maintain the balance between the continuous power extracted from the photovoltaic modules with the power injected into the grid by the inverter. (Teodorescu et al., 2011).

$$C_{(P+Res)damp.} = \underbrace{2}_{P} + \left[\underbrace{\frac{200 * 754s}{s^2 + 754s + 10^2}}_{Res}\right] \quad (1)$$

The voltage control loop of the DC bus uses control technique with PI controller, as expressed in the transfer function in Equation (2) (Souza, Borges, Santos, & Macedo, 2018). Next to it, the control of the inverter powers is based on the instantaneous power theory. The instantaneous values for P and Q are subtracted from the corresponding reference powers, where P_{ref} is the real active power produced by the module and Q_{ref} is the idle capacity of the inverter. Note that Q_{ref} is given by Equation (3), where S_{nom} is the nominal apparent power of the inverter.

$$C_v = 0.09041\left(\frac{s + 93.2}{s}\right) \quad (2)$$

$$Q_{ref} = \sqrt{S_{nom}^2 - P^2} \quad (3)$$

It is worth noting that the improvement proposed by this control is proportional and based on Equation (3).

Then, the resulting P and Q powers will be handled by PI controllers (where Kp = 0.003 and Ki = 0.3), these values were presented by (Teodorescu et al., 2011) and changed by the authors to better suit this work, for each of the powers. First of all, the active portion subtracts from the variable resulting from the DC voltage control, to generate the reference current i_d that is controlled to manage the active power, in order to perform voltage regulation on the DC bus.

The reactive power, after PI control, will correspond to the reference current i_q which is controlled to manage the reactive power exchange, in order to keep the power management in the inverter always at 1 p.u. (per unit). It is important to note that, for the reason of obtaining a unit power factor, the product between (Q_{ref} *x Cont_Q*) must be equal to zero during normal inverter operation. After determining the variables i_d and i_q, both are converted to i_α and i_β, respectively, and added to the current control (Teodorescu et al., 2011). Finally, these are converted to the abc domain to generate the pulses by PWM and sent to the IGBT switches, LCL filter and the power grid.

Overview of the proposed control for SDVV/MVD

When a fault (short circuit in the power grid) occurs, the voltage in the PCC drops; this voltage reduction spreads close to the point of disturbance. In this sense, there is a possibility the voltage level violates the appropriate limits defined by ANEEL in PRODIST in its module 8, as shown in Table 7 - Classification of Short-Duration Voltage Variation (ANEEL, 2018b, p. 20). This table indicates the duration and amplitude of the voltage variation, which compels the inverter to immediately switch from normal operation to SDVV operating mode. It is also worth mentioning that the SDVV control strategy improved in this work has a big difference in relation to the other methods described in the introduction.

The main difference is based on the voltage recovery process during the fault time, which consists of injecting amounts of active and reactive power depending on the amplitude of the sag. This process continues until the grid protection isolates the fault or even before the anti-islanding protection disconnects the inverter from the grid.

Inspired by the limits established by ANEEL PRODIST module 8 (ANEEL, 2018b), then, Table 1 will be a reference to establish the voltage levels at which the adopted control will acting.

Table 1. Voltage ranges applied to the SDVV control.

Designation	Duration of Variation	Voltage amplitude (RMS value) range with respect to the nominal voltage
Momentary Voltage Dip (MVD)	Greater than or equal to one cycle and less than or equal to three seconds	$0.1\ V_{nom} \leqslant V < 0.9\ V_{nom}$

Figure 3 represents the control strategy to minimize the effects of the SDVV/MVD, which is applied during the sag. A logic unit for sag detection (Fault Detection) is added to the control topology. This unit has the characteristic of perceiving the voltage variations of the grid and checking if they are within the limits established by Table 1. If the voltages are below 0.9 of the nominal value, the system changes from normal operation (OP) to operation mode in SDVV. In this situation, the control methodology also uses the AVR strategy established by IEEE 421.5-2005 DC1A (IEEE, 2006), where V_t is the grid voltage measured in p.u. and V_{ref} is the reference voltage equal to 1 p.u.

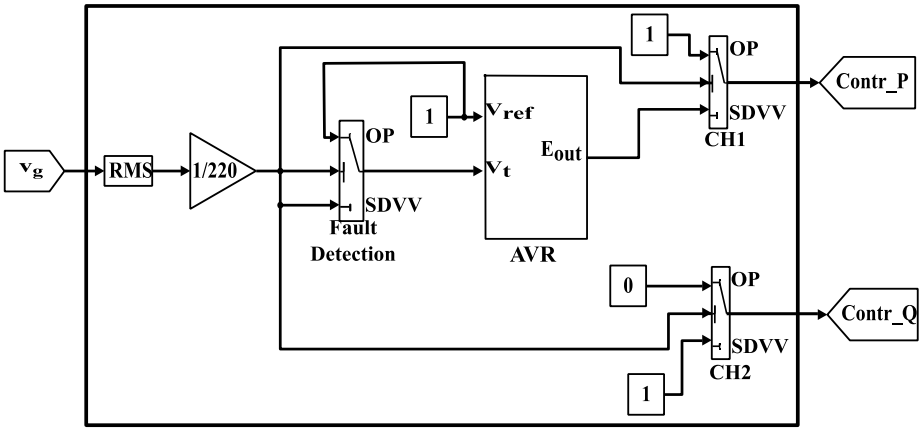

Figure 3. Schematic diagram for SDVV/MVD control proposal.

In this context, once the voltage sag is detected, exceeding the pre-set limit in the control according to Table 1, the control signal of the AVR output is multiplied by the inverter function. In the sequence sent into the CH1, which presents the same condition as the "Fault Detection", that is, if the voltage in the PCC is below

0.9 p.u. the operation will be in the SDVV condition, so Contr_P will receive the control signal. In this way, the proposed strategy will enter into the operating mode that will consequently decrease the injection of active power and increase the injection of reactive power in the power grid, as shown in Figure 2. The variable Contr_Q in 1, that is, the condition of CH2 it was established (V_{nom} <*0.9* p.u.), the condition of injecting reactive into the power grid will be enabled. In this condition of grid fault, the variables Contr_P and Contr_Q, which are integrated with the remaining of the control as shown in Figure 2, will cause the inverter to balance the injection of powers (increase of reactive power and reduction of active power). In this way, the control will be contributing to the reduction of the voltage sag and making it possible that possible loads sensitive to SDVV are not disconnected from the distribution power grid.

Still on the control shown in Figure 2, it is known that when the voltage in the PCC decreases to a value less than 0.9 p.u. of the rated voltage, then the inverter control will be switched to the SDVV condition. It is noteworthy that while the voltage is between 0.1 to 0.9 p.u. de V_{nom}, the output value of the AVR (control signal - *Contr_P*), will be multiplied by the reference value (P_{ref}) of the active power supplied by the photovoltaic array. Hence, the more severe the voltage sag is, the lower the active power injected by the inverter into the power grid will be. With this, there will be an idle space in the capacity to manage power in the inverter to inject reactive energy into the grid. In this way, Q_{ref} identifies the amount of reactive power that can be supplied by the inverter, thus contributing to alleviate the voltage sag.

It is worth mentioning that, the proposed control defines the reactive reference power Q_{ref} respecting the Equation (3). Otherwise, if there is no grid fault, the value of Q_{ref} is multiplied by *Contr_Q* set to zero to maintain a unit power factor during normal operating mode.

The operational strategy of the proposed SDVV/MVD control is shown in the flowchart of Figure 4.

The control is based on the constant voltage reading in the PCC and when the MVD condition is satisfied ($0.1\ V_{nom} \leqslant V < 0.9\ V_{nom}$), the Contr_P and Contr_Q signals are generated by the "Proposed control" block. In this block, the Contr_P output signal has a value between 1 and 0 (making the active power decrease) and the Contr_Q output signal becomes equal to 1 (enabling reactive power injection). Next, these signals are treated by their respective PI compensators, being the P_Control and the Q_Control, soon after, they are converted to the stationary reference system (α-β), generating the i_{α}^{*} and i_{β}^{*}, which are compared to the i_{α} and i_{β} of the grid. Finally, the signals resulting from the comparison are handled by the P+Res compensators and sent to the PWM to perform the inverter switching in this mode of operation. On the other hand, when there is no voltage sag, the control acts normally, that is, it injects only active power (depending on the climatic conditions), as described in the flowchart above.

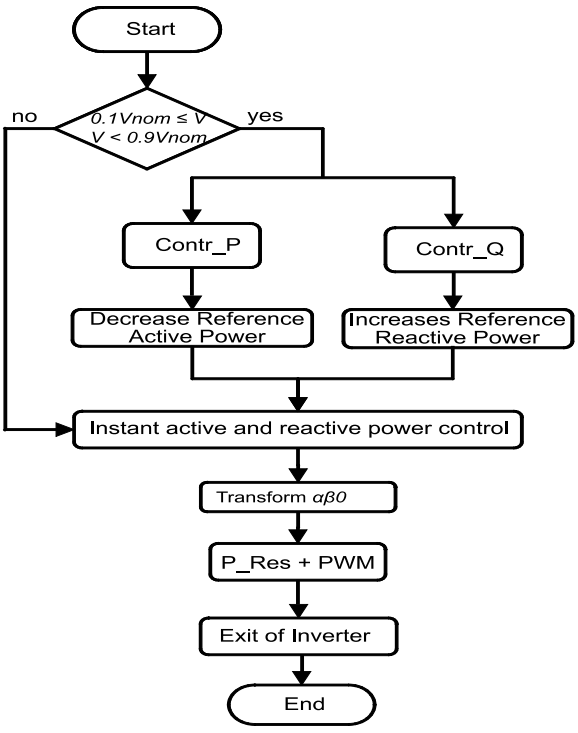

4. Flowchart of the SDVV/MVD control strategy.

Power grid distributed

More details on the power grid used for the simulations can be found in (Piccini et al., 2014; 2021; Rivera Sanhueza & Leal Freitas, 2018). This grid is a real power grid, located in block 1106 South in Palmas, capital of the state of Tocantins, Brazil. This block has the following characteristics: 1427 consumer units (residences, companies, public agencies or industries), served through three-phase delta-star distribution transformers with nominal powers of 75 kVA, 112.5 kVA and 150 kVA, and a voltage ratio of 13.8 kV:380/220 V. It is noteworthy that the grid loads in question are all three-phase.

The single-line diagram for the site in question is shown in Figure 5. It is important to note that the 13.8 kV primary distribution grid feeds the transformers through feeder 2 of the Palmas III substation. In addition, the consumer units connected to each secondary transformer are added up and represented as a single load. The data related to the aerial distribution grid, interconnections, transformers and loads are detailed in (Piccini et al., 2021).

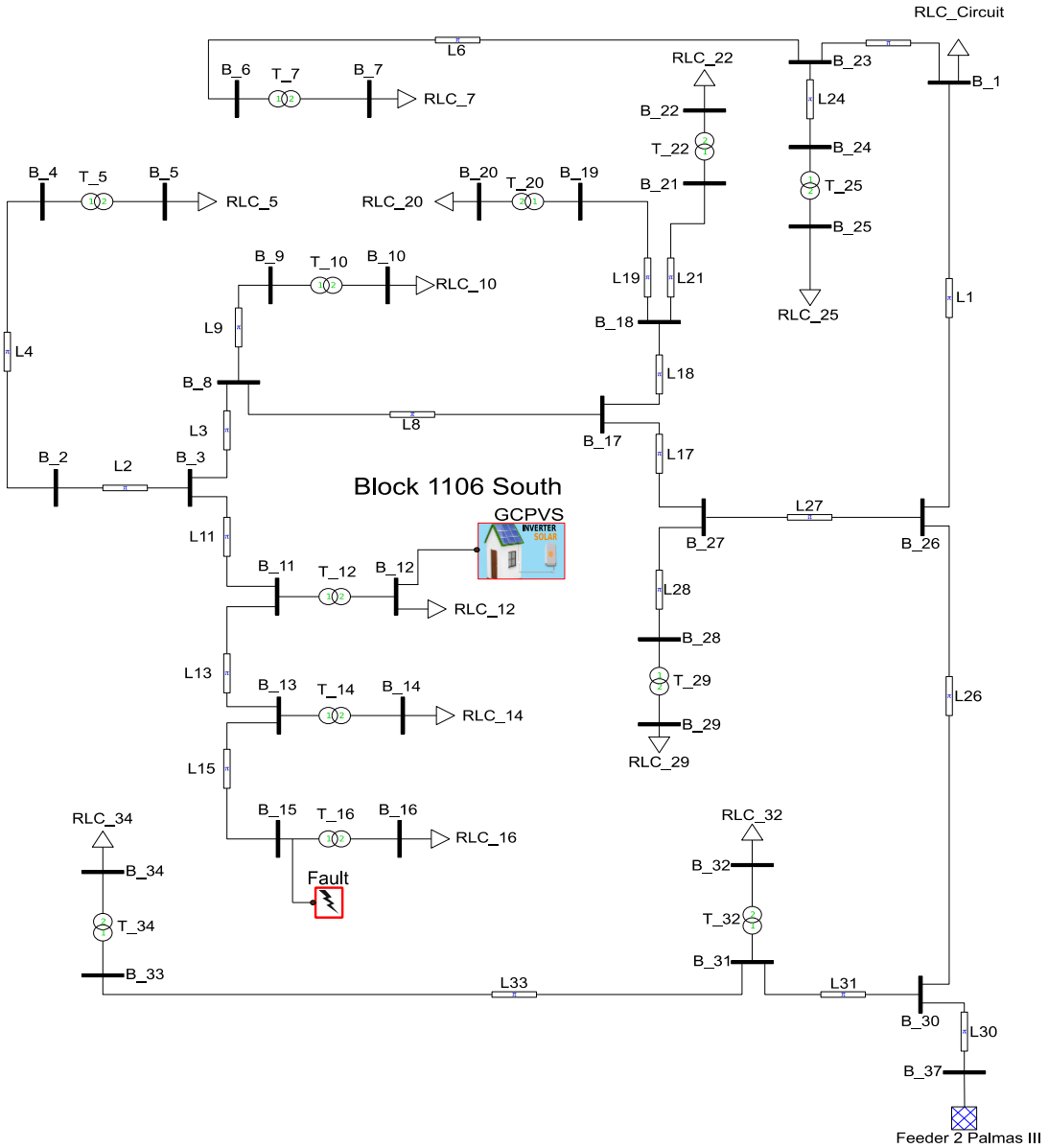

Figure 5. Single-line diagram of the real grid modeled in Matlab/Simulink®.

Results and discussion

The complete GCPVS model used to test the proposed SDVV/MVD control was implemented on the Matlab / Simulink® computing platform. For the case study, it was chosen a time of greater consumption of electricity in the distribution grid of Palmas and without the presence of photovoltaic DG. Thus, likewise

aforementioned, the collected data, such as voltages, currents, powers and power factors are actual measurements provided by the local electric utility. For this condition, the readings were: the magnitude of the voltage of 13.63 kV, and powers of 2.6815 MW, 1.5907 MVAr and 3.1178 MVA (FP = 0.8601) in feeder 2 of Palmas III. All of these data were included in the simulation.

Then, the GCPVS was connected to the three-phase secondary transformer T_12 and the values of voltage, current and instantaneous power were measured in PCC B_12.

In order to meet the SDVV requirements established in Brazilian standards, the proposed control will keep the GCPVS connected, injecting the available amount of active and reactive power to mitigate the voltage sag, in the same way, previously described. It is important to mention that ANEEL has not allowed yet neither 75 kW photovoltaic systems to remain connected when there is a fault of synchronism with the network, nor that they contribute with auxiliary services into the distribution power grid.

From now on, the results of the GCPVS dynamic voltage support for SDVV will be shown.

The behavior of the three-phase voltages in the PCC, bus B_12, which is connected to the secondary transformer T_12 and the load RLC_12, represents the sum of all consumer units connected to this transformer, which together add up to a power of 48.156 kW and 28.574 kVAr. It was found that the voltage levels on the secondary transformer are 366.5/211.6 V, which are below the nominal voltage, since the substation voltages are also below 13.8 kV, around 13.63 kV, and this condition is reflected throughout the system. The values of the voltages in the secondary of T_12 are plotted for four situations: in the first, without DG, in the second with 1 DG, in the third with 2 DGs connected in parallel and finally, in the fourth situation with 3 DGs connected in parallel. It is worth remembering that each GCPVS has a power of 75 kW and in the irradiance condition of 1 kW/m², being connected to bus B_12 (PCC), where it connects the secondary of T_12 and in parallel the RLC_12 load. Therefore, this location was chosen due to presenting a possibility of expansion of the photovoltaic system, on account of, in this location there is a municipal school and a public area destined to the free market.

Phase-to-ground fault

A phase-to-ground short-circuit (fault or failure) in phase B has been inserted into the distribution power grid at bus B_15, consequently, there will be a voltage sag in the vicinity of bus B_15. This fault had a duration of 0.625 s, that is, more than 20 cycles, likewise not only determined by ANEEL in module 8 of PRODIST (ANEEL, 2018b), but also presented by (Al-Shetwi et al., 2018).

For the purpose of better visualization, the voltages Va, Vb and Vc were plotted in the 4 separate situations, shown in Figure 6(a), (b) and (c) respectively. It is important to highlight that phase A suffered the greatest voltage sag at the time of the fault, for all situations presented. This happens due to the transformer connections, where the primary is in Delta (D1) and the secondary in Grounded Star (Yg) (Dy7 connection). There is a reversal in phases as presented in IEC 60076-1, for this transformer connection (International Electrotechnical Commission [IEC], 2000).

In the first situation (without DG) the behavior of the three-phase RMS voltages at the time of the fault is similar for phases A and B showing a voltage sag, while for phase C a slight increase in voltage, as shown in Figure 6(a), (b) and (c). It was possible to verify that, before the fault, the voltages are at 211.6 V, when the fault arises in the time of 1 to 1.625s, there will be a difference between the amplitudes. After it, the amplitudes will return to the pre-fault condition, as shown in Table 2.

From the second situation, where there are DG connections on the B_12 bar, before the failure, the voltages are in the desired range, that is, greater than 0.9 p.u. of the nominal voltage (V_{nom} = *220 V* phase-neutral). Thus, the inverter will remain connected without the injection of any reactive power, while the active power will remain in full generation according to the climatic conditions.

At the time of the fault, in an attempt to assist the operation of the improved control and balance the powers, the active power will be reduced with the aid of the AVR Figure 7(a). As a result, the reactive power injection capacity will be greater, Figure 7(b), contributing to sustain the voltage level in the B_12 bar, where the DGs are connected. Therefore, for the second situation (with 1 DG), before the fault, the voltages have an amplitude around 214.6 V, during the failure phase A measured a voltage at 155.3 V, while phase B at 186 V and phase C at 219.7 V, according to Table 2.

In the sequence, in the third situation (with 2 DGs), before the fault, the voltages have an amplitude around 217.4 V, while at the time of sag, the voltages increase to 163 V, 193.3 V and 227.2 V for phase A, B and C, respectively.

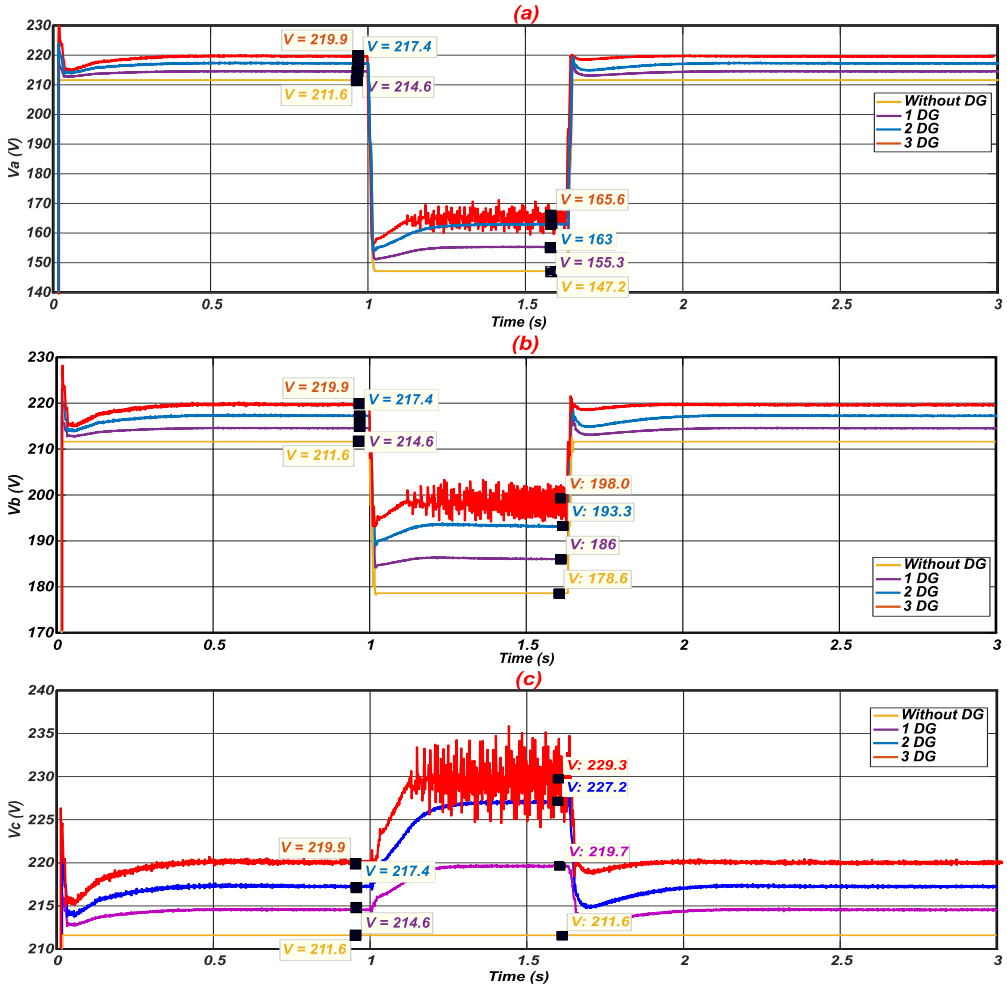

Figure 6. Voltages for each of the four simulations: (a) Va, (b) Vb, (c) Vc.

Table 2. Voltages for Va, Vb and Vc, without and with the insertion of the DG during the fault.

Voltages	Without DG	1 DG	2 DG	3 DG
Va (V)	147.2	155.3	163.0	165.6
Vb (V)	178.6	186.0	193.3	198.0
Vc (V)	211.6	219.7	227.2	229.3
Voltages p.u.	0.814	0.851	0.886	0.898

Finally, in the fourth situation (with 3 GDs totaling 225 kW), it is verified that before the fault, the voltages of the power grid are practically equal to V_{nom} = 219.9 V. In the occurrence of the sag, there is a high power for the installed location; the voltages in phases A, B and C undergo oscillations due to the AVR acting. Once the average voltage reaches the set point of 0.9 p.u., the control stops its action. But as the fault still exists, the control is trying to recover voltages to the best possible levels. Consequently, the average voltages for Va, Vb and Vc are 165.6 V, 198 V and 229.3 V, respectively. It was possible to notice that in phase C there were overvoltage peaks lasting 1 semi-cycle, as the proposed control compensates equally for the three phases.

Figure 8 shows the average of the three-phase voltage in p.u. before, during and after the voltage sag. It was found that only in the fourth situation, with a large amount of power being injected location into the power grid, the average voltage during the sag oscillated in the value of 0.9 p.u., which represents the set point of the control action. With that, it was possible to verify the full functioning of the proposed improvement.

In Figure 7, the behavior and the balance of the active and reactive powers are verified. During the fault, the active power decreases for the inverter to inject reactive power, in order to contribute to the voltage support in the PCC, as this operation eases the voltage sag.

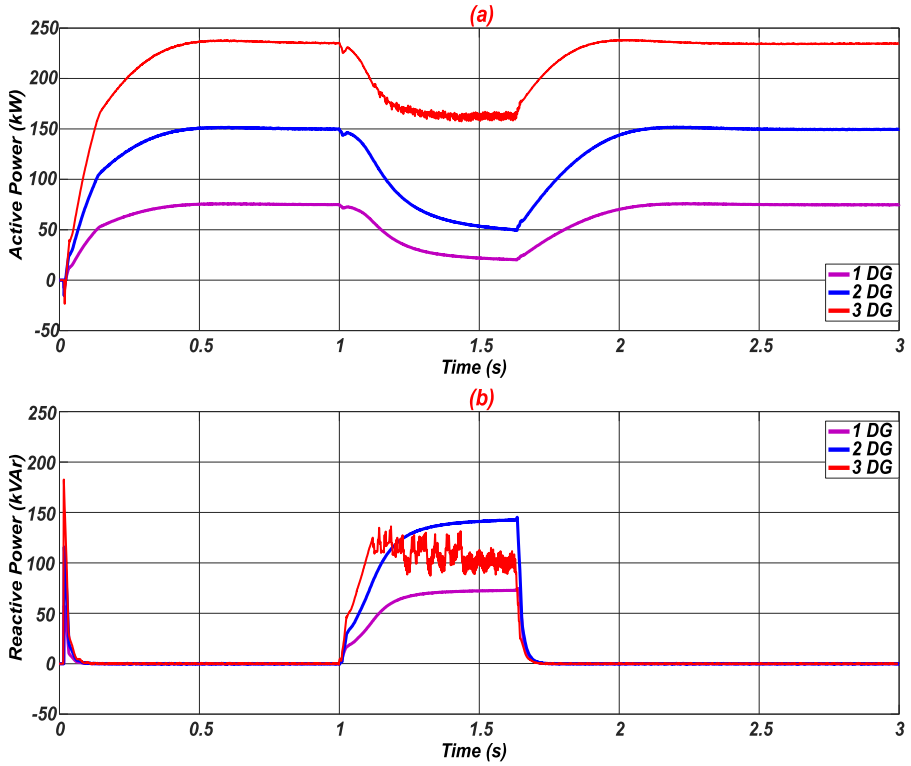

Figure 7. Powers in each of the situations: (a) Active, (b) Reactive.

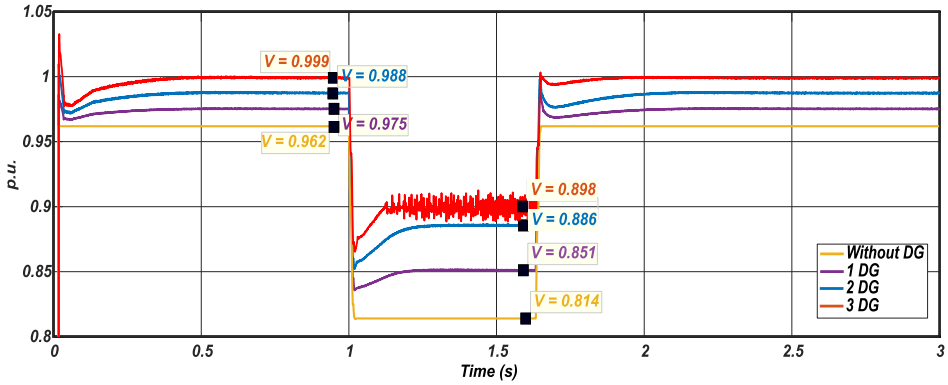

Figure 8. Average three-phase voltage in p.u. for each of the situations.

Two-phase-to-ground fault

Following this, a new short-circuit study was simulated. For this situation, it will be between two-phase-to-ground, (Phase B-C-to-ground). Respecting the previous conditions of the short-circuit time and location. The behavior of the stresses for the 4 new situations is shown in Figure 9, further described by Table 3.

Table 3. Voltages for Va, Vb and Vc, without and with the insertion of the DG during the two-phase-to-ground fault.

Voltages	Without DG	1 DG	2 DG	3 DG
Va (V)	171.6	182.8	192.8	201.7
Vb (V)	57.77	69.52	80.79	91.16
Vc (V)	161.1	169.2	176.4	182.4
Voltages p.u.	0.59	0.63	0.68	0.72

It was verified that before and after the fault the voltages are the same as those presented in the previous tests. At the time of fault, they exhibit different behaviors. All 3 phases undergo sag in their voltage levels, phase B being the most impaired, then phase C and lastly, phase A suffering less from the voltage sag. It is also possible to visualize the control performance for each situation. In addition, with the insertion of 3 DGs has the best condition to support the voltage levels. There are no overvoltage for any of the phases, as

presented in the previous study. Nevertheless, the average voltage in p.u. does not approach the set point, so the control operates the entire time of the short-circuit.

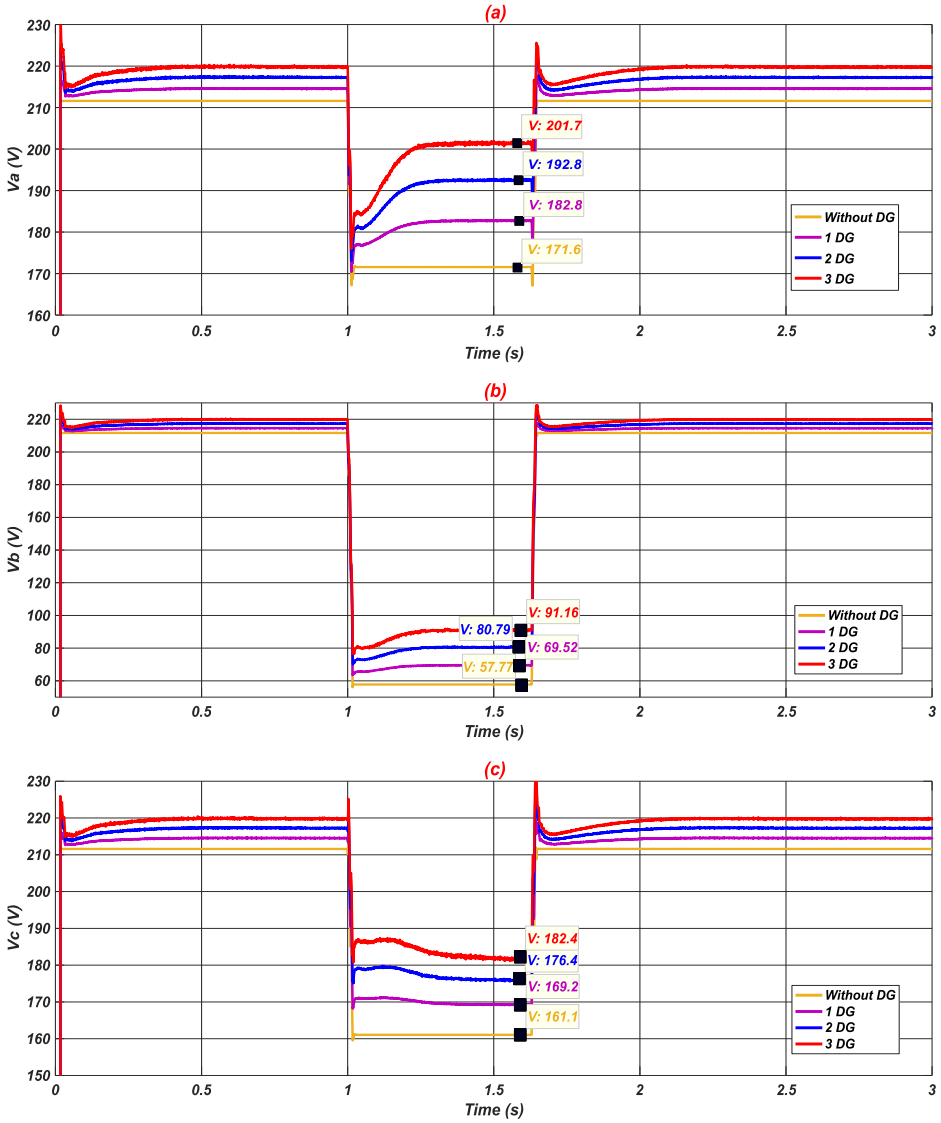

Figure 9. Voltages for each of the four simulations for the two-phase-to-ground fault: (a) Va, (b) Vb, (c) Vc.

Figure 10 shows the behavior of the active and reactive powers. It was found that even with the insertion of 3 DGs, the control finds a balance between the injection of active and reactive power. It quickly decreases the active power and, consequently, increases the reactive power to try to bring the voltage to the appropriate levels.

Finally, for the purpose of demonstrating the behavior of the voltage on the GCPVS DC bus, Figure 11 presents the graph of the response to the two individually explored events (phase-to-ground and two-phase-to-ground faults).

During faults, the DC bus voltage approaches the value of the open-circuit voltage of the PV array (V_{oc} = 1046 V), and this can compromise the performance and life of the DC bus capacitor, so it is suggested that the installed capacitor supports the full open-circuit voltage of the array. The graphs of the DC bus voltage, for the two analyzed situations, show that the voltages do not exceed the value of the open-circuit voltage, since the proposed GCPVS is of a single stage without the use of a boost converter.

It was possible to verify that this paper proposes a photovoltaic system connected to the grid with a control strategy for short-duration voltage variation, momentary voltage dip (SDVV/MVD) for low voltage three-phase distribution power grid. The method is based on the strategy of automatic voltage regulators (AVR), normally used by synchronous power generators. The control balances the injection of active and reactive power for the reason of helping to support the voltage levels of the grid at the time of fault. Although the regulation of the Brazilian agency ANEEL has not allowed small photovoltaic systems to make such contributions yet, some researches have already been carried out for the scientific community associated to this aim.

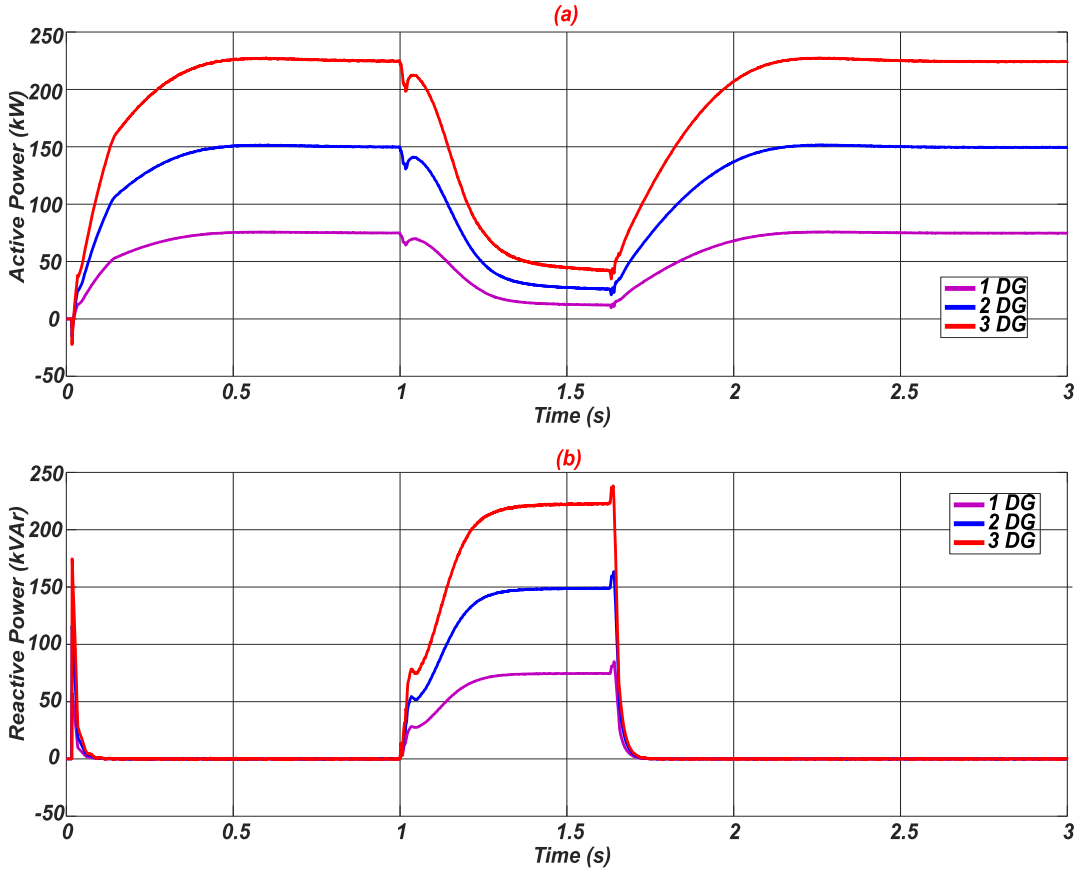

Figure 10. Powers in each of the situations to two-phase-to-ground fault: (a) Active, (b) Reactive.

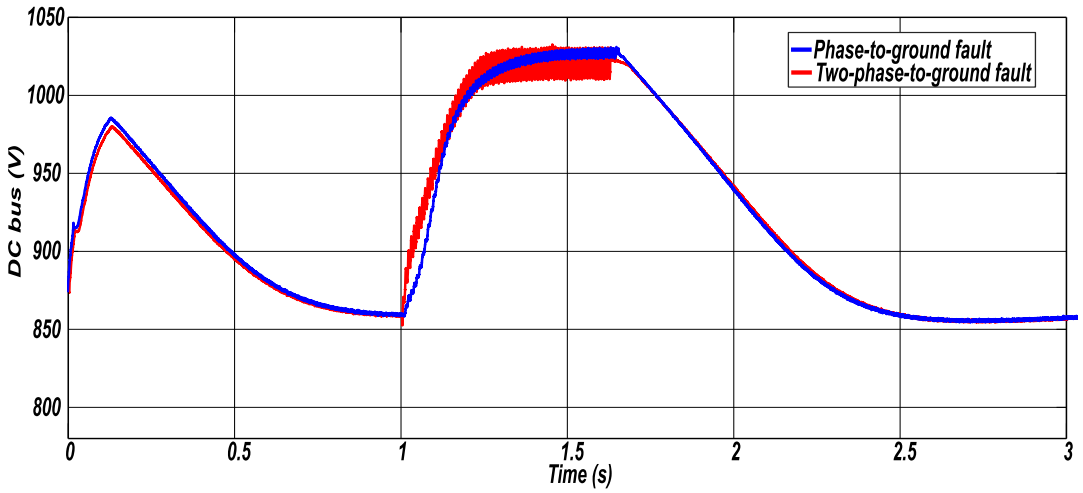

Figure 11. DC bus voltage for the two faults.

Finally, it was possible to verify that even in the situation of short-circuit between phase B-to-ground, with 3 DGs totaling 225 kW, with a large amount of photovoltaic power inserted in a place where the demand for power loads is 48.156 kW and 28.574 kVAr. The proposed control is able to improve the voltage level for all phases, even fluctuating in its set point value. It was also identified that less reactive power was needed to the end of helping to support voltage levels.

For the second study, two-phase-to-ground short-circuit, there was an improvement in the voltage levels of all phases. It was observed that for phase A there was an improvement of more than 30 V or 17 %, for phase B that presented the most severe sag the voltage increased by more than 33 V or 57 % and finally, phase C more than 21 V or 13 %. It was found that it would be interesting to perform the powers compensation applied at each one of the three phases separately, to better deal with voltage sags situations caused by asymmetrical faults.

Conclusion

Finally, it was proved that not only with the proposed control but also with the greatest penetration of the most efficient DG are the voltage support for the presented faults.

It would also be possible for small PVS to offer some ancillary services into the power grid, under abnormal conditions. It was possible to verify that, under normal conditions, the AVR does not interfere with the operation of the GCPVS.

Moreover, for continuity of work and future work, demonstrate the simulations for even more severe voltage sag as symmetrical three-phase fault and insert more DGs into the modeled power grid.

Acknowledgements

This work was supported by two Brazilian public higher education institutions: Federal Institute of Paraná - Campus Paranavaí (IFPR) and Federal University of Uberlândia (UFU).

References

Afshari, E., Moradi, G. R., Yang, Y., Farhangi, B., & Farhangi, S. (2017). A review on current reference calculation of three-phase grid-connected PV converters under grid faults. In *Proceedings of the 2017 IEEE Power and Energy Conference at Illinois* [PECI], (p. 1–7). DOI: https://doi.org/10.1109/PECI.2017.7935761

Agência Nacional de Energia Elétrica [ANEEL]. (2018a). *Geração distribuída.* Recovered on August 3, 2020 from https://www.aneel.gov.br/geracao-distribuida.

Agência Nacional de Energia Elétrica [ANEEL]. (2018b). *PRODIST-Módulo 8: Procedimentos de distribuição de energia elétrica no sistema elétrico nacional – PRODIST*. *Qualidade da energia elétrica*. Recovered on August 3, 2020 from https://www.aneel.gov.br/modulo-8

Agência Nacional de Energia Elétrica [ANEEL]. (2021). *Procedimentos de distribuição de energia elétrica no sistema elétrico nacional-PRODIST*. Recovered on August 3, 2020 from https://www.aneel.gov.br/prodist

Albuquerque, F. L., Moraes, A. J., Guimarães, G. C., Sanhueza, S. M. R., & Vaz, A. R. (2010). Photovoltaic solar system connected to the electric power grid operating as active power generator and reactive power compensator. *Solar Energy*, *84*(7), 1310–1317. DOI: https://doi.org/10.1016/j.solener.2010.04.011

Al-Shetwi, A. Q., Sujod, M. Z., & Blaabjerg, F. (2018). Low voltage ride-through capability control for single-stage inverter-based grid-connected photovoltaic power plant. *Solar Energy*, *159*, 665–681. DOI: https://doi.org/10.1016/j.solener.2017.11.027

Ammar, M., & Sharaf, A. M. (2019). Optimized use of PV distributed generation in voltage regulation: a probabilistic formulation. *IEEE Transactions on Industrial Informatics*, *15*(1), 247–256. DOI: https://doi.org/10.1109/TII.2018.2829188

Caetano, L., Caaixeta, G., Lima, T., Oliveira, J., Ramos, R., & Rodrigo, A. (2019). Modelling of a multipurpose photovoltaic generator block using ATP-EMTP. *IEEE Latin America Transactions*, *17*(2), 203–209. DOI: https://doi.org/10.1109/TLA.2019.8863165

Comerio, A., Scarpart, T. T., Krause, R. C. K., Fernandes, M. R., & Muniz, P. R. (2020). Performance of photovoltaic generators under superficial dust deposition on their modules derived from anthropogenic activities. *Acta Scientiarum. Technology*, *43*(1), e50101. DOI: https://doi.org/10.4025/actascitechnol.v43i1.50101

Goqo, Z., & Davidson, I. E. (2018). A review of grid tied PV generation on LV distribution networks. In *Proceedings of the 2018 IEEE PES/IAS PowerAfrica*, (907–912). DOI: https://doi.org/10.1109/PowerAfrica.2018.8521039

International Electrotechnical Commission [IEC]. (2000). *Annex D: Three-Phase Transformer Connections*. *In* IEC (Eds.), *International standard IEC 60076-1, Power transformers—Part 1: General (Ed. 2.1 2000-04)* (p.81-86). Geneva, SW: IEC. Recovered on August 10, 2020 from https://bitlybr.com/3PgGVr

Institute of Electrical and Eletronics Engineers [IEEE]. (2006). IEEE recommended practice for excitation system models for power system stability studies. *IEEE Std 421.5-2005 (Revision of IEEE Std 421.5-1992)*, 1–93. DOI: https://doi.org/10.1109/IEEESTD.2006.99499

Institute of Electrical and Eletronics Engineers [IEEE]. (2018). IEEE standard for interconnection and interoperability of distributed energy resources with associated electric power systems interfaces. *IEEE Std 1547-2018 (Revision of IEEE Std 1547-2003)*, 1–138. DOI: https://doi.org/10.1109/IEEESTD.2018.8332112

Instituto Nacional de Eficiência Energética [INEE]. (2020). *O que é Geração Distribuída*. Recovered on August 3, 2020 from http://www.inee.org.br/forum_ger_distrib.asp

Jinko Solar. (2020). *Jinko Solar*. Cheetah JKM390-410M-72H-(V)-A4-EN-F30. Retrieved on August 3, 2020 from https://www.jinkosolar.com/uploads/Cheetah%20JKM390-410M-72H-(V)-A4-EN-F30.pdf

Kabalcı, E. (2020). Review on novel single-phase grid-connected solar inverters: circuits and control methods. *Solar Energy*, *198*, 247–274. DOI: https://doi.org/10.1016/j.solener.2020.01.063

Michels, R. N., Canteri, M. G., Silva, M. A. d. A. e, Gnoatto, E., Santos, J. A. A. d., & Jesus, M. M. A. d. (2015). Yield from photovoltaic modules under real working situations in west Paraná-Brazil. *Acta Scientiarum. Technology*, *37*(1), 19–24. DOI: https://doi.org/10.4025/actascitechnol.v37i1.19191

Mishra, M. K., & Lal, V. N. (2020). An improved methodology for reactive power management in grid integrated solar PV system with maximum power point condition. *Solar Energy*, *199*, 230–245. DOI: https://doi.org/10.1016/j.solener.2020.02.001

Piccini, A. R., Guimarães, G. C., Souza, A. C., & Denardi, A. M. (2021). Implementation of a photovoltaic inverter with modified automatic voltage regulator control designed to mitigate momentary voltage dip. *Energies*, *14*(19), 6244. DOI: https://doi.org/10.3390/en14196244

Piccini, A. R., Tamashiro, M. A., Rodrigues, A. R., Guimarães, G. C., & Barbosa, C. S. (2014). Steady state analysis of a medium/low voltage distribution grid behavior with PV system penetration. In *Proceedings of the International Conference on Renewable Energies and Power Quality* [ICREPQ´14], (p. 532–537). DOI: https://doi.org/10.13140/2.1.2067.6484

Reznik, A., Simões, M. G., Al-Durra, A., & Muyeen, S. M. (2014). LCL filter design and performance analysis for grid-interconnected systems. *IEEE Transactions on Industry Applications*, *50*(2), 1225–1232. DOI: https://doi.org/10.1109/TIA.2013.2274612

Rivera Sanhueza, S. M., & Leal Freitas, S. C. (2018). Overvoltage forecast in a urban distribution power grid considering PV systems conection. *IEEE Latin America Transactions*, *16*(8), 2221–2227. DOI: https://doi.org/10.1109/TLA.2018.8528238

Safayet, A., Fajri, P., & Husain, I. (2017). Reactive power management for overvoltage prevention at high PV penetration in a low-voltage distribution system. *IEEE Transactions on Industry Applications*, *53*(6), 5786-5794. DOI: https://doi.org/10.1109/TIA.2017.2741925

Souza, A. C. d., Borges, D. T. d. S., Santos, I. N., & Macedo, J. R. (2018). Evaluation of linear current control methods in single-phase grid-tie inverters. *IEEE Latin America Transactions*, *16*(5), 1424–1431. DOI: https://doi.org/10.1109/TLA.2018.8408437

Sufyan, M., Rahim, N. A., Eid, B., & Raihan, S. R. S. (2019). A comprehensive review of reactive power control strategies for three phase grid connected photovoltaic systems with low voltage ride through capability. *Journal of Renewable and Sustainable Energy*, *11*(4), 042701. DOI: https://doi.org/10.1063/1.5095185

Teodorescu, R., Liserre, M., & Rodriguez, P. (2011). *Grid Converters for Photovoltaic and Wind Power Systems*. Hoboken, NJ: Wiley.

Wen, H., & Fazeli, M. (2019). A low-voltage ride-through strategy using mixed potential function for three-phase grid-connected PV systems. *Electric Power Systems Research*, *173*, 271–280. DOI: https://doi.org/10.1016/j.epsr.2019.04.039